Circular RNA hsa_circ_0001666 sponges miR-330-5p, miR-193a-5p and miR-326, and promotes papillary thyroid carcinoma progression via upregulation of ETV4

YING QI[1], JINGNI HE[2], YING ZHANG[3], LIDONG WANG[2], YIFAN YU[2], BAIYU YAO[2] and ZHONG TIAN[2]

Departments of [1]Radiology, [2]General Surgery and [3]Clinical Oncology,
Shengjing Hospital of China Medical University, Shenyang, Liaoning 110022, P.R. China

Received October 12, 2020; Accepted January 28, 2021

DOI: 10.3892/or.2021.8001

Abstract. Circular RNAs (circRNAs) are a group of regulators that affect the aggressive behaviors of several types of cancer. Hsa_circ_0001666 (also referred to as hsa_circ_000742) is a newly discovered circRNA that is upregulated in human papillary thyroid carcinoma (PTC) based on microarray analysis. However, the role of hsa_circ_0001666 in PTC progression remains unknown. Thus, the aim of the present study was to determine the potential function and underlying mechanism of hsa_circ_0001666 in PTC. The results demonstrated that hsa_circ_0001666 was upregulated in both PTC clinical samples and cell lines. Its expression was associated with lymph node metastasis of patients with PTC. Knocking down hsa_circ_0001666 expression inhibited cell proliferation, as evidenced by decreased cell viability, arrest of cell cycle progression at the G_1 phase and an increase in cell cycle-associated proteins. Apoptosis rates and expression levels of pro-apoptotic proteins were also increased by silencing hsa_circ_0001666. In xenograft experiments, the oncogenic effect of hsa_circ_0001666 on tumor growth was verified. Additionally, luciferase reporter assays showed that hsa_circ_0001666 and ETS variant transcription factor 4 (ETV4) shared common binding sites with three microRNAs [(miRNA/miR)-330-5p, miR-193a-5p and miR-326]. Knockdown of these miRNAs separately reversed the inhibitory effect of hsa_circ_0001666 small interfering RNAs on PTC tumor aggressiveness, and ETV4 overexpression also induced a similar effect to that of miRNA inhibitors. Thus, hsa_circ_0001666 may function as an oncogene, promoting PTC tumorigenesis via the miR-330-5p/miR-193a-5p/miR-326/ETV4 pathway. This provides a basis for identifying potential novel therapeutic targets for PTC.

Correspondence to: Professor Jingni He, Department of General Surgery, Shengjing Hospital of China Medical University, 39 Huaxiang Road, Tiexi, Shenyang, Liaoning 110022, P.R. China
E-mail: jingnihe@foxmail.com

Key words: papillary thyroid carcinoma, hsa_circ_0001666, microRNAs, ETS variant transcription factor 4, sponge

Introduction

Thyroid carcinoma (TC) is an endocrine carcinoma with increasing incidence worldwide in 2018 (1). Papillary TC (PTC) is a differentiated type of TC that accounts for ~80% of all cases of TC (2). The majority of patients with PTC have a favorable prognosis with a ~90% overall survival rate due to the improvements in therapeutic strategies, such as surgical excision, radiotherapy and hormone suppression (3). Targeted treatments provide novel insights into the mechanism underlying PTC progression, such as the use of tyrosine kinase inhibitors (4). Small-molecule MAPK inhibitors increase the susceptibility of PTC cells to radioiodine (5). Nevertheless, certain patients still exhibit a poor prognosis due to the presence of distant metastasis. Thus, developing novel therapeutic targets is essential for limiting PTC progression.

Circular RNAs (circRNAs) are the most recently discovered type of non-coding RNA generated by the back-splicing of precursor mRNAs with covalently closed loop structures (6). These are extensively expressed in eukaryotes and have been shown to participate in multiple biological processes, including sponging microRNAs (miRNA/miRs), interacting with RNA-binding proteins and regulating gene expression levels (7-9). Previous studies have reported that circRNAs exhibit tumor promoting or suppressive effects in several types of cancer, such as hepatocellular carcinoma, glioma and lung adenocarcinoma (10-12). Additionally, in PTC, the dysregulated expression of circRNAs is responsible for several adverse clinicopathological features, such as capsular infiltration, advanced pathological T stage and lymph node metastasis (13). Liu *et al* (14) demonstrated that circRap guanine nucleotide exchange factor 5 (RAPGEF5) serves a tumorigenic role in PTC via the miR-198/FGFR1 axis. Microarray analysis has shown that a novel circRNA hsa_circ_0001666 (hsa_circ_000742), derived from the linear gene family with sequence similarity (FAM)120B, is upregulated in PTC (15). To the best of our knowledge, however, the biological functions of hsa_circ_0001666 in PTC have not been studied.

miRNAs are evolutionarily conserved small non-coding RNAs that regulate multiple biological processes. Several miRNAs, such as miR-221, miR-146b-5p and miR-1178, have been reported to modulate PTC development and progression (16-18). For example, miR-206 suppresses drug resistance to Euthyrox by targeting MAP4K3 (19). A recent study showed that miR-330-5p mediates the positive regulation of long intergenic non-protein-coding RNA 003311 on cancer stem-like features in PTC (20). miR-326 suppresses PTC cell proliferation and metastasis by inhibiting MAPK1 and erb-b2 receptor tyrosine kinase (ERBB) 4 (21).

ETS variant transcription factor 4 (ETV4) serves a tumor promoting role in non-small-cell lung, breast and pancreatic cancer (22-24). The present study aimed to discover potential common binding miRNAs with hsa_circ_0001666 and ETV4. Emerging evidence indicates that circRNAs may sponge miRNAs to regulate gene expression levels (14,25). However, whether hsa_circ_0001666 serves as a miRNA sponge in PTC remains unknown.

The expression of hsa_circ_0001666 in PTC and its biological functions were here investigated. A miR-330-5p/miR-193a-5p/miR-326/ETV4 axis was used to elucidate the regulatory mechanism of hsa_circ_0001666.

Materials and methods

Clinical samples. Patients with PTC (n=60, female and male; age, 28-71 years) were enrolled at Shengjing Hospital of China Medical University (Shenyang, China) between April 2019 and June 2020. The distance between tumor and matching normal adjacent tissue was ~2 cm. Patients who were diagnosed with PTC for the first time and with no prior treatment history associated with cancer were included. Patients who received prolonged hormonotherapy or immunosuppressive therapy were excluded. In addition, patients with complicated chronic diseases, pregnant or lactating women, and children were also excluded. All tissues samples were collected and immediately frozen in liquid nitrogen for further examination. The present study was approved by the Institutional Review Board of Shengjing Hospital of China Medical University and performed in accordance with the Declaration of Helsinki. All patients provided written informed consent. The collected tumor tissues and adjacent normal tissues were used to measure hsa_circ_0001666 expression levels and analyze the associations between hsa_circ_0001666 and clinicopathological features.

Cell culture. Three human PTC cell lines, TPC-1 (Procell Life Science & Technology Co., Ltd.), IHH-4 (CoBioer Biosciences Co., Ltd.) and GLAG-66 (Guangzhou Cellcook Biotech Co., Ltd.), and human thyroid follicular epithelial cell line Nthy-ori 3-1 (Shanghai Zhongqiaoxinzhou Biotech) were obtained. All cell lines were STR profiled every year if no other problems were reported. Mycoplasma testing was also performed every 3 months. TPC-1 and Nthy-ori 3-1 cells were cultured in RPMI-1640 medium (Sigma-Aldrich; Merck KGaA). GLAG-66 cells were cultured in DMEM (Sigma-Aldrich; Merck KGaA). IHH-4 cells were incubated in DMEM/RPMI-1640 (Sigma-Aldrich; Merck KGaA) mixed medium. All media were supplemented with 10% FBS (Sigma-Aldrich; Merck KGaA) and the cells were cultured at 37˚C in a humidified incubator with 5% CO_2.

Fluorescence in situ hybridization (FISH). FISH staining was performed to determine the cellular distribution of hsa_circ_0001666 using a FISH kit (Guangzhou RiboBio Co., Ltd.). TPC-1 cells were seeded in a 24-well plate ($3x10^4$ cells/well) and fixed in 4% paraformaldehyde at room temperature for 10 min. Then, specific FISH probes against hsa_circ_0001666 were used to hybridize its junction site. The nuclei were counterstained with DAPI (0.005 mg/ml) at room temperature for 10 min. 18S probes were used as the positive control. Images of FISH staining were captured using a light Olympus microscope (Olympus Corporation) at x400 magnification.

Reverse transcription (RT)PCR. TPC-1 cells ($2x10^5$/well) were plated in 6-well plates. For RNase R treatment, total RNAs were extracted from TPC-1 cells and incubated in the presence or absence of RNase R (Guangzhou Jisai Biological Technology Co., Ltd.) at 37˚C for 30 min and subsequently reverse-transcribed using Super M-MLV Reverse Transcriptase kit (BioTeke Corporation) according to the manufacturer's protocol at 42˚C for 50 min. Genomic (g)DNA from cells was isolated using a genome DNA isolation kit (BioTeke Corporation) according to the manufacturer's protocol. The complementary (c)DNA or gDNA was analyzed by RT-PCR using specific primers (Table SII); PCR products were separated on a 1.5% agarose gel and analyzed using Sanger sequencing (Sangon Biotech Co., Ltd.).

Cell transfection. For hsa_circ_0001666 knockdown, five pairs of small interfering (si)RNAs against hsa_circ_0001666 and corresponding negative control (NC) siRNA (JTS Scientific Ltd.) were constructed and transfected into TPC-1 or IHH-4 cells at a final concentration of 23 nM for 48 h.

For miRNA overexpression, miR-330-5p, miR-193a-5p, miR-326 or corresponding NC mimics (JTS Scientific Ltd.) were transfected into PTC cells for 48 h at a concentration of 23 nM.

In addition, miR-330-5p, miR-193a-5p, miR-326 or corresponding NC inhibitors were acquired from JTS Scientific Ltd. The ETV4 overexpression plasmid or empty vector was constructed by GenScript. For the rescue experiments, TPC-1 cells were co-transfected with hsa_circ_0001666 siRNAs (23 nM) and miRNA inhibitor (23 nM) or NC inhibitor for 48 h. ETV4 overexpressing pcDNA3.1 vector or empty pcDNA3.1 vector at a final concentration of 455 ng/ml together with hsa_circ_0001666 siRNAs (23 nM) were transfected into TPC-1 cells for 48 h.

All oligonucleotide sequences (Table SI) were transfected into PTC cells using Lipofectamine® 2000 (Invitrogen; Thermo Fisher Scientific, Inc.) following the manufacturer's instruction at room temperature. All subsequent experiments were performed at 48 h post transfection. The transfection efficiency for inhibiting gene expression was ~70% and for overexpressing gene expression was ~900%.

Cell Counting Kit (CCK)8 assay. CCK8 assays were performed to investigate the viability of cells (Beyotime Institute of Biotechnology). In brief, TPC-1 or IHH-4 cells were seeded

in a 96-well plate ($4x10^3$ cells/well) and incubated with CCK8 solution (10 μl) for 1 h. A microplate reader was used to measure the absorbance at 450 nm.

5-ethynyl-2'-deoxyuridine (Edu) staining assay. An Edu assay kit (Nanjing KeyGen Biotech Co., Ltd.) was utilized to assess cell proliferation. Briefly, transfected TPC-1 and IHH-4 cells ($3x10^4$/well) were collected and incubated with Edu reagent according to the manufacturer's protocol. Subsequently, cells were counterstained with Hoechst 33342 (1:2,000) for 15 min at room temperature, harvested and observed under a light microscope at x400 magnification.

Flow cytometry. Cells were seeded onto 6-well plates ($2x10^5$ cells/well). After transfection for 48 h, cells were collected to determine cell cycle distribution or cell apoptosis. For cell cycle analysis, cells were pre-treated with 70% cold ethanol at 4˚C overnight and incubated with PI solution for 30 min at 4˚C in the dark according to the manufacturer's protocol (Nanjing KeyGen Biotech Co., Ltd.). Cell apoptosis was measured using Annexin V-FITC/PI apoptosis detection kit (Nanjing KeyGen Biotech Co., Ltd.). Flow cytometry instrument NovoCyte (ACEA Bioscience, Inc.) was used to detect the cells and NovoExpress 1.3.4 software (ACEA Bioscience, Inc.) was used to analyze data.

Luciferase reporter assay. Bioinformatics analysis predicted that hsa_circ_0001666 was complementary to three miRNAs (miR-330-5p, miR-193a-5p and miR-326) based on StarBase v3.0 (starbase.sysu.edu.cn/index.php) and Circular RNA Interactome software (circinteractome.nia.nih.gov/index.html). In addition, these three miRNAs were predicted to bind with ETV4 3'-UTR based on StarBase. In order to confirm this association, wild-type and mutant sequences of the targeting region of hsa_circ_0001666 or ETV4 were constructed and cloned into a pmirGLO vector (Promega Corporation). Subsequently, 293T cells were co-transfected with the wild-type or mutant luciferase reporter plasmids targeting hsa_circ_0001666 or ETV4, together with miR-330-5p, miR-193a-5p or miR-326 mimics using Lipofectamine® 2000 (Invitrogen; Thermo Fisher Scientific, Inc.) for 48 h. Binding activity was measured using a Dual luciferase reporter assay kit (Promega Corporation), relative to firefly/Renilla luciferase activity.

RNA binding protein immunoprecipitation (RIP) assay. RIP experiments were performed using a Magna RIP RNA-Binding Protein Immunoprecipitation kit (EMD Millipore) according to the manufacturer's protocol. TPC-1 and IHH-4 cell lysates were incubated with argonaute RISC catalytic component 2 (AGO2) antibody stock solution (cat. no. 10686-1-AP; Wuhan Sanying Biotechnology) for 30 min at room temperature, and relative hsa_circ_0001666 expression levels were determined by RT-quantitative (q)PCR.

Animal experiments. Animal care was performed in line with the Guide for the Care and Use of Laboratory Animals (26) and all experiments were approved by Shengjing Hospital of China Medical University. A total of 24 male BALB/c nude mice (age, 4 weeks; weight, 14-16 g) were purchased from Beijing HFK Bioscience Co., Ltd. and housed in a 12-h light/dark cycle with a humidity of 45-55% at 22±1˚C, and had free access to food and water. Briefly, TPC-1 or IHH-4 cells with hsa_circ_0001666 expression stably knocked down or stably expressing sh-NC cells at density of $1x10^7$ in 100 μl RPMI-1640 or DMEM/RPMI-1640 (both Sigma-Aldrich; Merck KGaA) per mouse were subcutaneously injected into the right side of the axilla of nude mice. Tumor size was measured every 4 days and calculated as length x $width^2$ x 0.5. The maximum tumor size was <0.5 cm^3. All mice survived during experiments. Mice were sacrificed at 28 days by injecting sodium pentobarbital (200 mg/kg) intraperitoneally and tumor tissue was harvested.

Histological analysis. The xenograft tumors were fixed in 4% paraformaldehyde for 48 h at room temperature. After being embedded in paraffin, the xenograft tumors were sectioned into 5-μm slices for histological examination. For cell apoptosis analysis *in vivo*, tissue sections were blocked in 3% H_2O_2 for 10 min at room temperature. TUNEL staining was performed using an *in situ* Cell Death Detection kit (Roche Diagnostics) according to the manufacturer's protocols. For cell proliferation analysis *in vivo*, the sections were blocked in goat serum stock solution (Beijing Solarbio Science & Technology Co., Ltd.) for 15 min at room temperature and incubated with primary antibody against Ki67 (1:100; cat. no. A2094; Abclonal Biotech Co., Ltd.) in PBS overnight at 4˚C, and then labeled horseradish peroxidase (HRP)-conjugated goat anti-rabbit secondary antibody (1:500; cat. no. 31460; Thermo Fisher Scientific, Inc.) in PBS was applied for 1 h at 37˚C. After counterstaining with hematoxylin (Beijing Solarbio Science & Technology Co., Ltd.) for 3 min at room temperature. the slices were visualized using a light microscope to observe three fields of view at x400 magnification.

RT-qPCR. Total RNA from all PTC cell lines, clinical tumor, adjacent normal or xenograft tumor tissues were extracted using TRIpure (BioTeke Corporation) and reverse-transcribed into cDNA using a Super M-MLV Reverse Transcriptase kit (BioTeke Corporation) according to the manufacturer's procedure at 42˚C for 50 min. RT-qPCR was performed using SYBR Green (Sigma-Aldrich; Merck KGaA). The thermocycling conditions for hsa_circ_0001666 were as follows: 94˚C for 5 min, 40 cycles of 94˚C for 15 sec, 60˚C for 25 sec and 72˚C for 30 sec. The thermocycling conditions for miRNAs were as follows: 94˚C for 4 min, 40 cycles of 94˚C for 15 sec, 60˚C for 20 sec and 72˚C for 15 sec. The thermocycling conditions for FAM120B and ETV4 were as follows: 94˚C for 5 min, 40 cycles of 94˚C for 15 sec, 60˚C for 25 sec and 72˚C for 30 sec. The relative expression levels of hsa_circ_0001666, miR-330-5p, miR-193a-5p, miR-326, FAM120B and ETV4 were determined using the $2^{-\Delta\Delta Ct}$ method (27). β-actin was used as the internal control for circRNA and mRNA and U6 was used as the internal control for miRNA. The relative gene expression levels in cell lines and xenograft tumors were normalized to the control. All primer sequences are listed in Table SII.

Western blotting. Total proteins from TPC-1 and IHH-4 cells or tissues were isolated using cell lysis buffer and quantified using

a BCA assay kit (both Beyotime Institute of Biotechnology). Equal quantities of proteins (20 μl) were loaded on 12 or 15% SDS-PAGE gel and transferred to a PVDF membrane (EMD Millipore). After blocking in 5% non-fat milk for 1 h at room temperature, membranes were incubated with primary antibodies against cyclin D1 (1:1,000; cat. no. A19038; Abclonal Biotech Co., Ltd.), cyclin E (1:1,000; cat. no. AF0144; Affinity Biosciences), Caspase-3 (1:1,000; cat. no. A19654), Caspase-9 (1:1,000; cat. no. A2636), ETV4 (1:1,000; cat. no. A5797) or β-actin (1:10,000; cat. no. AC004; all Abclonal Biotech Co., Ltd.) in 5% non-fat milk dilution overnight at 4˚C. Membranes were incubated with HRP-conjugated goat anti-rabbit (1:5,000; cat. no. A0208) or goat anti-mouse secondary antibodies (1:5,000; cat. no. A0216; Beyotime Institute of Biotechnology) in 5% non-fat milk for 45 min at 37˚C. Protein signals were visualized with an ECL kit (Beyotime Institute of Biotechnology), captured and analyzed using Gel-Pro-Analyzer 4.0 software (Media Cybernetics, Inc.).

Statistical analysis. Data were presented as mean ± SD. Differences between groups were compared using unpaired Student's t-test or one-way ANOVA followed by post hoc Bonferroni's correction using GraphPad Prism 8.0 software (GraphPad Software, Inc.). Comparisons of hsa_circ_0001666 expression levels between clinical tumors and adjacent normal tissues were analyzed by paired Student's t-test. Associations between hsa_circ_0001666 expression level and clinicopathological features were analyzed using Chi-square or Fisher's exact test. The numbers of independent repeats for each experiment were as follows: *In vitro,* three; *in vivo*, six; CCK8, five; RIP and RT-qPCR, three. $P<0.05$ was considered to indicate a statistically significant difference.

Results

Identification and expression of hsa_circ_0001666 in PTC and clinical significance. Dysregulated expression of circRNAs has been reported to be involved in tumor progression (10). Through microarray analysis, a novel circRNA, hsa_circ_0001666, has previously been found to be significantly upregulated in human PTC tumors (15). In order to validate whether exons 2, 3 and 4 of the FAM120B gene formed hsa_circ_0001666 (Fig. 1A), divergent and convergent primers were designed to amplify hsa_circ_0001666 and FAM120B. hsa_circ_0001666 was detected by the divergent primers in cDNAs in the presence or absence of RNase R treatment, but not in gDNA from PTC cells; by contrast, the linear FAM120B mRNA amplified by convergent primers was absent in cDNA following RNase R treatment (Fig. 1B). Sanger sequencing of the PCR products further confirmed the back-splicing junction of hsa_circ_0001666 (Fig. 1C), which supported the closed circular structure of hsa_circ_0001666. Furthermore, FISH staining showed that that hsa_circ_0001666 was primarily localized in the cytoplasm of PTC cells (Fig. 1D). Next, the expression of hsa_circ_0001666 in PTC was confirmed by RT-qPCR analysis. Results showed that hsa_circ_0001666 was significantly upregulated in PTC tissues compared with the adjacent normal specimens (Fig. 2A), consistent with results in the PTC cell lines (Fig. 2B). The association between hsa_circ_0001666 expression levels and clinicopathological features of patients with PTC were analyzed. The analysis showed that hsa_circ_0001666 expression level was associated with lymph node metastasis, but not with sex, age and tumor stage (Table I). These results highlighted the potential oncogenic role of hsa_circ_0001666 in PTC.

Silencing hsa_circ_0001666 inhibits cell proliferation and promotes apoptosis in vitro. In order to investigate the function of hsa_circ_0001666 in PTC cells, five specific siRNAs targeting hsa_circ_0001666 were prepared. Results showed that these siRNAs significantly decreased hsa_circ_0001666 expression levels but did not affect FAM120B mRNA expression levels (Fig. 2C and D). The two siRNAs (si-circ-1 and si-circ-2) with the most efficient interference ability were used for subsequent experiments.

The effect of hsa_circ_0001666 on cell proliferation was evaluated. Results from the CCK8 and Edu staining assays demonstrated that hsa_circ_0001666 knockdown significantly inhibited cell viability and proliferation (Fig. 3A and B). The cell cycle was arrested at the G_1 phase in TPC-1 and IHH-4 cells transfected with hsa_circ_0001666 siRNAs (Fig. 3C). Moreover, the expression levels of cell cycle-associated proteins (cyclins D1 and E) were significantly decreased in the transfected cells (Fig. 3D).

The role of hsa_circ_0001666 in the apoptosis of PTC cells was next assessed. Hsa_circ_0001666 knockdown promoted the apoptosis of PTC cells, as shown by flow cytometry analysis (Fig. 3E). Furthermore, the expression levels of pro-apoptotic proteins, including cleaved caspase 3 and caspase 9, were increased following knockdown of hsa_circ_0001666 in PTC cells (Fig. 3F). These results showed that hsa_circ_0001666 knockdown suppressed proliferation and promoted apoptosis of PTC cells *in vitro*.

Hsa_circ_0001666 directly regulates the miR-330-5p/miR-193a-5p/miR-326/ETV4 axis. Considering the cytoplasmic distribution of hsa_circ_0001666 in PTC cells, it was speculated that it may exert its functions by sponging miRNAs. In total, three potential miRNAs (miR-330-5p, miR-193a-5p and miR-326) were predicted to be complementary to hsa_circ_0001666 (Fig. 4A). The transfection efficiency for miR-330-5p, miR-193a-5p or miR-326 mimics is shown in Fig. S1A-C. Luciferase reporter assays demonstrated that miR-330-5p, miR-193a-5p or miR-326 mimics inhibited the luciferase activity of cells co-transfected with hsa_circ_0001666 wild-type plasmid. However, there were no statistically significant changes in the luciferase activity of cells co-transfected with the mutant hsa_circ_0001666 (Fig. 4B). RIP assays were performed to demonstrate a significant enrichment of AGO2 binding to hsa_circ_0001666 compared with IgG in TPC-1 and IHH-4 cells (Fig. 4C). Based on the predicted results, these three miRNAs were shown to have binding sites with ETV4 mRNA (Fig. 4D). Results suggested that the binding activity of the wild-type ETV4 was decreased by these miRNAs compared with the mutant ETV4 (Fig. 4E). It was also demonstrated that both the mRNA and protein expression levels of ETV4 were significantly downregulated by these three miRNAs (Fig. 4F and G). Therefore, the data illustrated that hsa_circ_0001666 shared a common binding

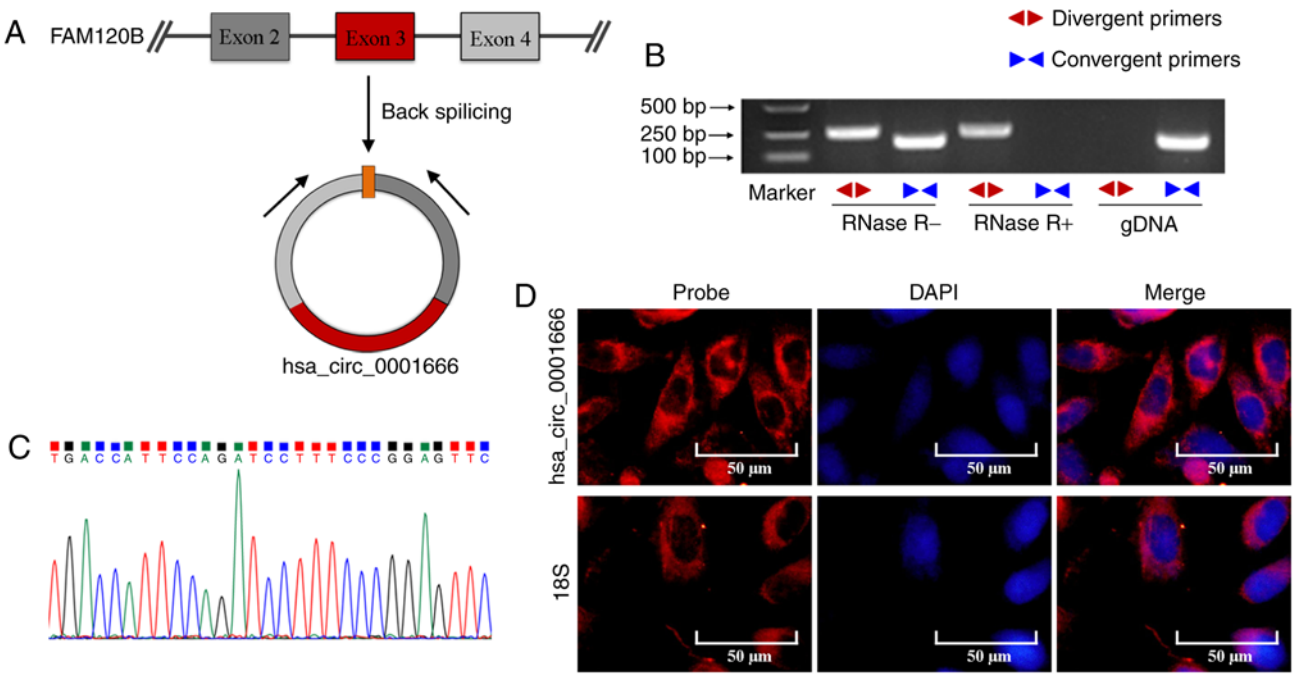

Figure 1. Hsa_circ_0001666 expression level analysis in papillary thyroid carcinoma cell lines. (A) Structural diagram of hsa_circ_0001666 showing that it is formed of exons 2, 3 and 4 of the FAM120B gene. (B) Reverse transcription PCR using divergent primers showed that hsa_circ_0001666 was present in complementary DNA but not in genomic DNA. (C) Sanger sequencing confirmed the back-splicing junction site of hsa_circ_0001666. (D) Fluorescence *in situ* hybridization analysis identified the cellular distribution of hsa_circ_0001666 in TPC-1 cells. FAM, family with sequence similarity.

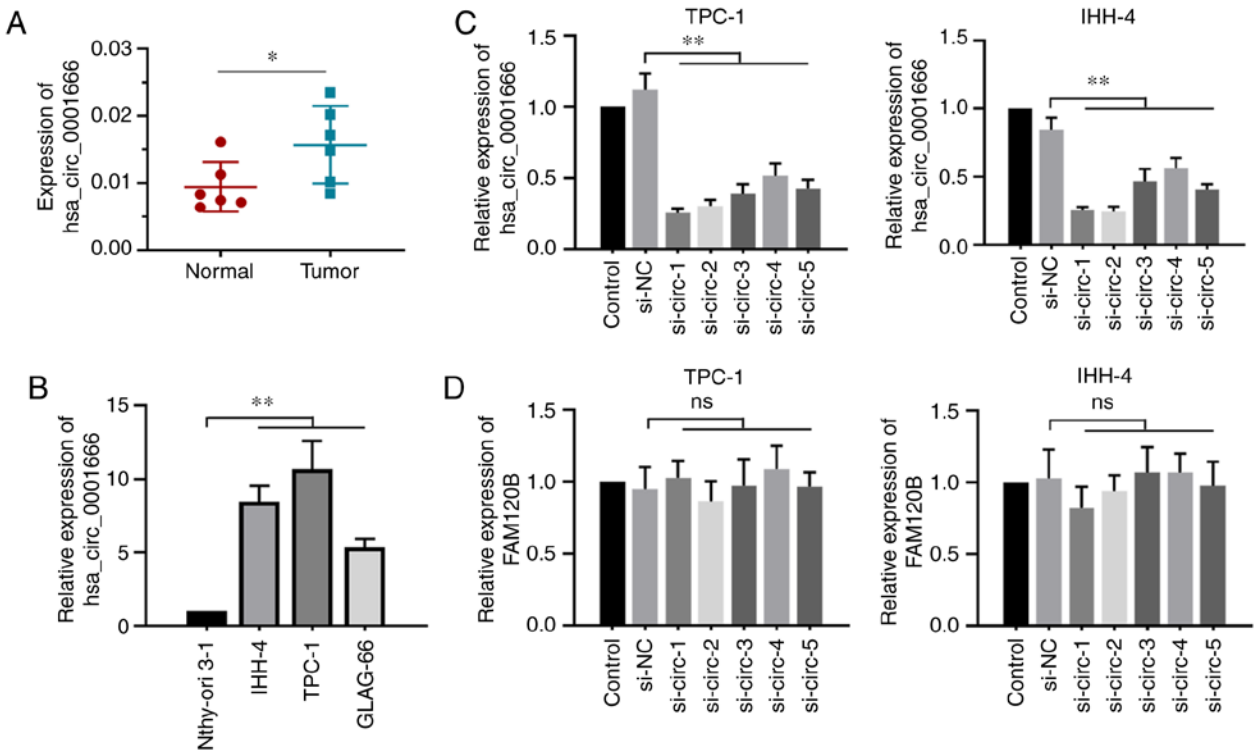

Figure 2. Expression levels of hsa_circ_0001666 in PTC tissue and cell lines. Reverse transcription-quantitative PCR showed that hsa_circ_0001666 was overexpressed in PTC (A) tissue and (B) cell lines and that the five pairs of hsa_circ_0001666 siRNAs (C) decreased its expression but (D) did not affect FAM120B expression levels in TPC-1 and IHH-4 cells. *P<0.05, **P<0.01. PTC, papillary thyroid carcinoma; si, small interfering; FAM, family with sequence similarity; ns, no significance; NC, negative control.

motif on miR-330-5p, miR-193a-5p and miR-326 with ETV4 and directly regulated the miR-330-5p/miR-193a-5p/miR-326 axis to upregulate ETV4 expression.

Hsa_circ_0001666 facilitates PTC cell growth by regulating the miR-330-5p/miR-193a-5p/miR-326/ETV4 axis. In order to determine whether the miR-330-5p/miR-193a-5p/miR-326/

Table I. Association between hsa_circ_0001666 expression levels and clinicopathological features of patients with papillary thyroid carcinoma.

		hsa_circ_0001666 expression levels		
Clinical parameter	Cases (n=60)	Low	High	P-value
Sex				
Male	11	7	4	
Female	49	23	26	0.5062
Age, years				
≤60	48	27	21	
>60	12	3	9	0.1042
Tumor stage				
T1	55	30	25	
T2-T4	5	0	5	0.0522
Lymph node metastasis				
N0	32	20	12	
N1	28	10	18	0.0384[a]

[a]P<0.05.

ETV4 axis mediated the effect of hsa_circ_0001666 on PTC cell proliferation and apoptosis, rescue experiments were performed. The transfection efficiency for miR-330-5p, miR-193a-5p or miR-326 inhibitor is presented in Fig. S1D-F. Specific inhibitors targeting miR-330-5p, miR-193a-5p or miR-326 resulted in upregulation of ETV4 following knockdown of hsa_circ_0001666 (Fig. 5A). The decreased cell viability and increased apoptosis in PTC cells with hsa_circ_0001666 knock down were reversed by these miRNA inhibitors (Fig. 5B and C). In addition, the role of ETV4 in regulation of hsa_circ_0001666 on PTC progression was further confirmed. Transfection of the ETV4 overexpression plasmid resulted in increased expression levels of ETV4 and also reversed the inhibitory effect of hsa_circ_0001666 knockdown on PTC cell proliferation (Fig. 5D and E). Moreover, the increased apoptotic rates were also suppressed by overexpression of ETV4 (Fig. 5F). Altogether, the data revealed that hsa_circ_0001666 targeted the miR-330-5p/miR-193a-5p/miR-326/ETV4 axis to promote PTC cell growth.

Silencing hsa_circ_0001666 inhibits tumor growth in vivo. TPC-1 or IHH-4 cells with hsa_circ_0001666 stably knocked down were injected into nude mice to determine the effect of hsa_circ_0001666 *in vivo*. Tumor sizes were significantly smaller in mice injected with by hsa_circ_0001666 knockdown cells (Fig. 6A). Knockdown of hsa_circ_0001666 induced a decrease in hsa_circ_0001666 expression levels and increased expression of miR-330-5p, miR-193a-5p and miR-326 in the tumors (Fig. 6B-E). Furthermore, a significant decrease in both ETV4 mRNA and protein expression levels was observed in the tumor tissue of mice injected with hsa_circ_0001666 knockdown cells (Fig. 6F and G). Histological analysis showed that hsa_circ_0001666 knockdown decreased Ki67 expression levels and increased the proportion of apoptotic cells in the xenograft tumors (Fig. 6H and I). The *in vivo* results supported the hypothesis that hsa_circ_0001666 exhibited an oncogenic effect on PTC tumor growth. The overall findings of the present study are summarized in Fig. 7.

Discussion

Abnormal expression of circRNAs in several types of cancer has been shown to serve an important role in aggressive tumor behavior, such as that of glioma, urothelial carcinoma and cervical cancer (25,28,29). The present study demonstrated that hsa_circ_0001666 expression was significantly upregulated in PTC tissue compared with matched adjacent normal tissue. In order to uncover the biological role of hsa_circ_0001666 and the underlying mechanism in PTC progression, loss-of-function experiments were performed using PTC cells and xenograft animals. Hsa_circ_0001666 knockdown suppressed proliferation and promoted apoptosis of PTC cells both *in vitro* and *in vivo*. The inhibitory effect of hsa_circ_0001666 silencing on PTC was reversed by miRNA inhibitors or ETV4 overexpression. The results suggested that hsa_circ_0001666 functioned as a sponge to mediate the miR-330-5p/miR-193a-5p/miR-326/ETV4 axis and promote PTC tumor progression.

Emerging evidence has shown that circRNAs are novel molecules associated with tumorigenesis, metastasis or drug resistance in PTC (30-32). It has previously been shown that circFOXM1 acts as a tumor promoter in PTC by regulating miR-1179/HMGB1 (33). Another circRNA, circRAPGEF5, was found to upregulate FGFR1 expression and facilitate PTC proliferation and metastasis via competitively binding with miR-198 (14). Microarray analysis by Peng *et al* (15) demonstrated that hsa_circ_0001666 expression is increased in PTC; this circRNA is located at chr6: 70726457-170739638.

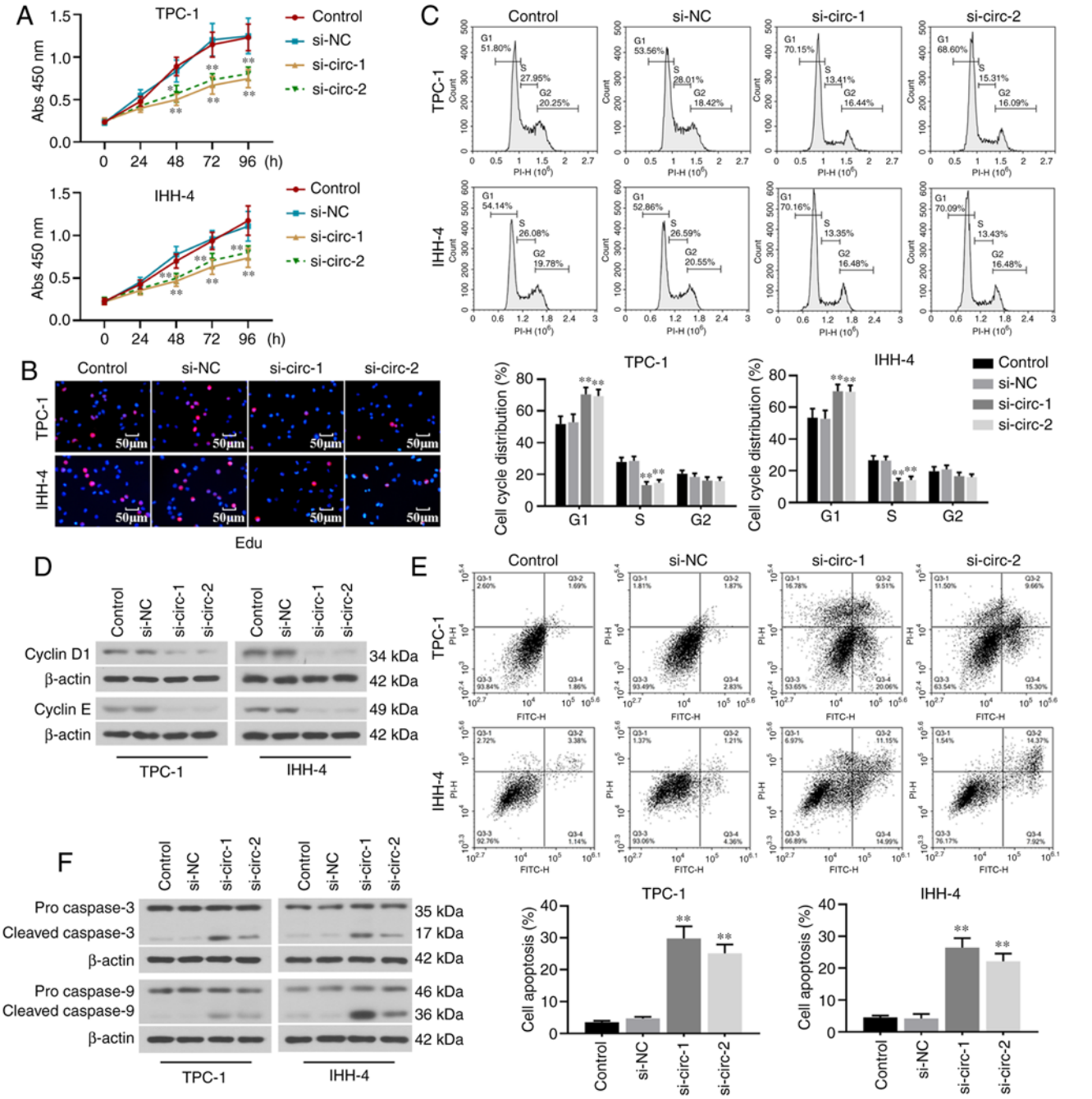

Figure 3. Knockdown of hsa_circ_0001666 inhibits cell proliferation and promotes apoptosis *in vitro*. (A) Cell viability was decreased by hsa_circ_0001666 siRNAs in TPC-1 and IHH-4 cells, as shown by Cell Counting Kit 8 assay. (B) 5-Ethynyl-2'-deoxyuridine staining showed that hsa_circ_0001666 knockdown decreased the proportion of cells in the S phase. (C) Knockdown of hsa_circ_0001666 arrested the cell cycle at the G_1 phase, as shown by flow cytometry analysis. (D) Protein expression levels of cyclin D1 and E were decreased by hsa_circ_0001666 silencing. (E) Hsa_circ_0001666 knockdown increased cell apoptosis, as shown by flow cytometry. (F) Protein expression levels of caspase-3, and caspase-9 were increased by hsa_circ_0001666 siRNAs. *P<0.05, **P<0.01 vs. si-NC. si, small interfering; NC, negative control; Abs, absorbance; circ, circular.

Bioinformatics analysis suggested that hsa_circ_0001666 functions as a sponge due to the presence of multiple miRNA binding sites in breast cancer (34). To the best of our knowledge, however, studies regarding the biological features of hsa_circ_0001666 have not been performed. The present study demonstrated that hsa_circ_0001666 was upregulated in PTC tissue and cell lines. Silencing hsa_circ_0001666 suppressed proliferation and G_1/S phase transition and promoted cell apoptosis *in vitro*. Similarly, downregulated expression levels of cell cycle proteins and upregulated expression levels of pro-apoptotic proteins were observed. Xenograft experiments confirmed the oncogenic effect of hsa_circ_0001666 on tumor growth *in vivo*.

circRNA-miRNA-mRNA interactions mediate tumorigenesis (35,36). Hsa_circ_0001666 was here shown to possess binding sites with three potential miRNAs (miR-330-5p, miR-193a-5p and miR-326). RIP assay confirmed the interaction between hsa_circ_0001666 and miRNAs. Luciferase reporter assays confirmed these three miRNAs directly bound with hsa_circ_0001666. These three miRNAs have

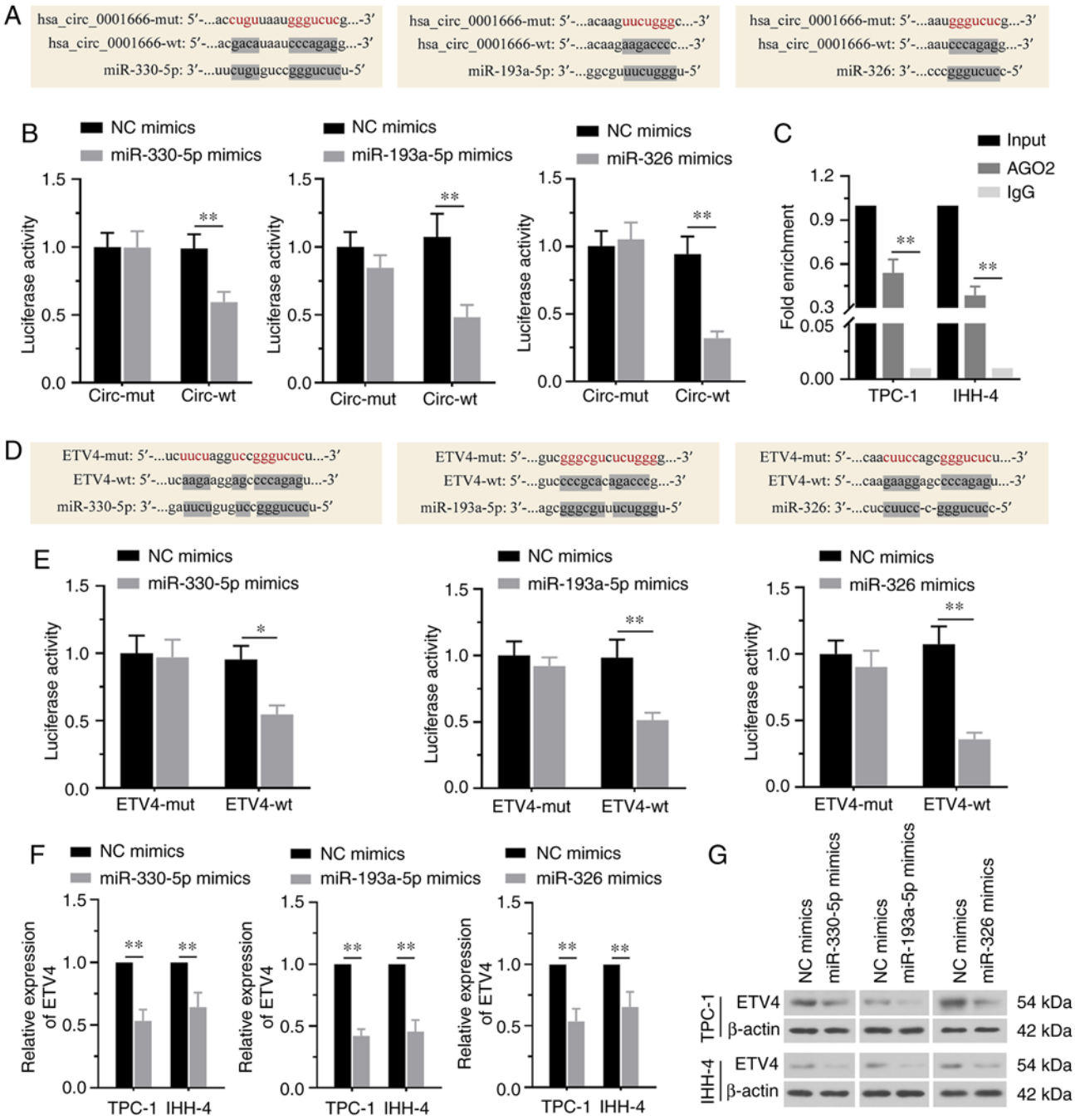

Figure 4. Hsa_circ_0001666 directly targets the miR-330-5p/miR-193a-5p/miR-326/ETV4 axis. (A) Sequence alignment of the binding sites between hsa_circ_0001666 and miR-330-5p, miR-193a-5p or miR-326. (B) Luciferase reporter assays showed that hsa_circ_0001666 directly bound to these miRs. (C) RNA binding protein immunoprecipitation analysis demonstrated that hsa_circ_0001666 bound to miRs. (D) Sequence alignment of the binding sites between ETV4 and miR-330-5p, miR-193a-5p or miR-326. (E) Luciferase reporter assays confirmed that miR-330-5p, miR-193a-5p, miR-326 targeted ETV4. (F) mRNA and (G) protein expression levels of ETV4 were decreased by the three miR mimics. *P<0.05, **P<0.01. miR, microRNA; ETV4, ETS variant transcription factor 4; mut, mutant; wt, wild-type; NC, negative control; circ, circular; AGO2, argonaute RISC catalytic component 2.

been investigated in various types of cancer. For example, miR-330-5p was shown to serve as a tumor suppressor in esophageal adenocarcinoma via regulating MMP1 (37). miR-326 inhibits the growth of breast cancer cells via regulating the ERBB/PI3K signaling pathway (38). miR-193a-5p directly targets SPOCK1 in hepatocellular carcinoma to repress its malignancy (39). Additionally, miR-330-5p and miR-326 have both been demonstrated to play tumor-suppressive roles in PTC progression (20,21). However, research on miR-193a-5p in PTC is limited. The present study showed that silencing miR-330-5p, miR-193a-5p or miR-326 using specific inhibitors negatively regulated the effect of hsa_circ_0001666 siRNAs on PTC cell proliferation and apoptosis.

It has been shown that miRNAs exert an important role in biological processes via regulating gene expression, such as miR-221 and miR-330-5p (16,37). In the present study, three miRNAs directly targeted ETV4, a transcriptional factor of E26 transformation-specific family, which is overexpressed in breast, lung and pancreatic cancer (22-24). Xu *et al* (40) showed that ETV4 bound to FOSL1 promoter to increase

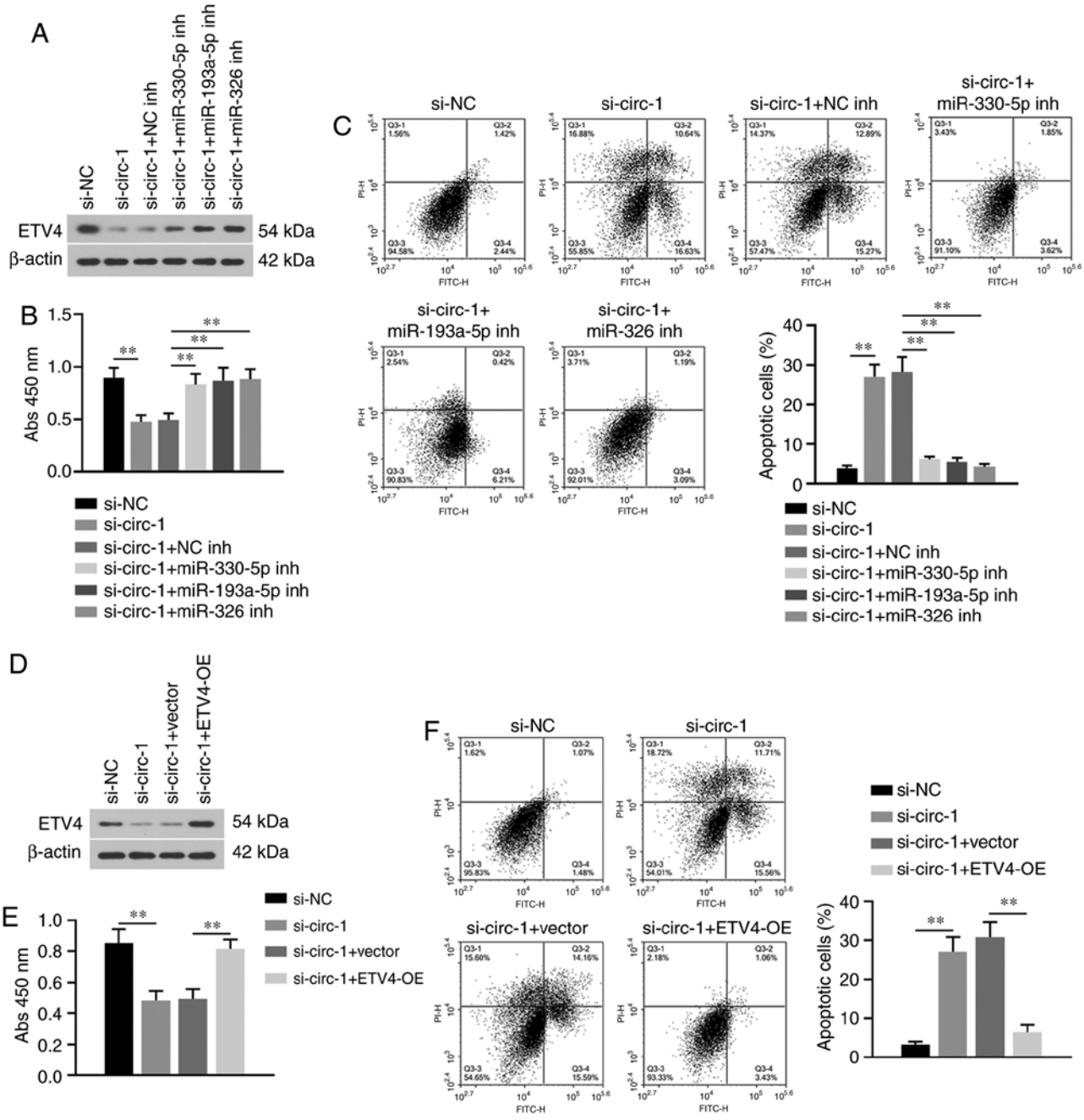

Figure 5. Hsa_circ_0001666 facilitates papillary thyroid carcinoma cell growth by regulating the miR-330-5p/miR-193a-5p/miR-326/ETV4 axis. TPC-1 cells were co-transfected with hsa_circ_0001666 siRNAs and miR-330-5p, miR-193a-5p or miR-326 inhibitor. Transfection with miR inhibitor (A) upregulated ETV4 protein expression, (B) increased viability and (C) inhibited apoptosis in cells transfected with hsa_circ_0001666 siRNA. TPC-1 cells were co-transfected with hsa_circ_0001666 siRNAs and ETV4 overexpression plasmids. ETV4 overexpression (D) upregulated ETV4 protein expression, (E) increased viability and (F) inhibited apoptosis in cells transfected with hsa_circ_0001666 siRNA. **P<0.01. miR, microRNA; ETV4, ETS variant transcription factor 4; si, small interfering; NC, negative control; circ, circular; inh, inhibitor.

cell migration in a PI3K/AKT-dependent manner in clear cell renal cell carcinoma. In hepatocellular carcinoma, ETV4 overexpression increases resistance to sorafenib and cisplatin to protect against apoptosis (41); it was also reported to be associated with the clinical response to MEK inhibitors in patients with melanoma (42), supporting its use as a potential biomarker in multiple types of cancer. The present study demonstrated that hsa_circ_0001666 silencing-induced effects on cell proliferation and apoptosis were reversed by ETV4 overexpression. Taken together, these data suggested that hsa_circ_0001666 serves as a sponge to promote tumor malignancy via the miR-330-5p/miR-193a-5p/miR-326/ETV4 pathway. In addition to ETV4, target genes, such as tripartite motif containing 25, transcription factor 3 and dual specificity phosphatase 28, were also identified to bind with the miRNAs in the present study. In future studies, the effect of these potential targets on the regulation of hsa_circ_0001666 in PTC progression should be assessed.

The present study has several limitations. For example, as a novel circRNA, data regarding hsa_circ_0001666 in cancer is limited. The present study showed that hsa_circ_0001666 functioned as an oncogene, promoting PTC progression both

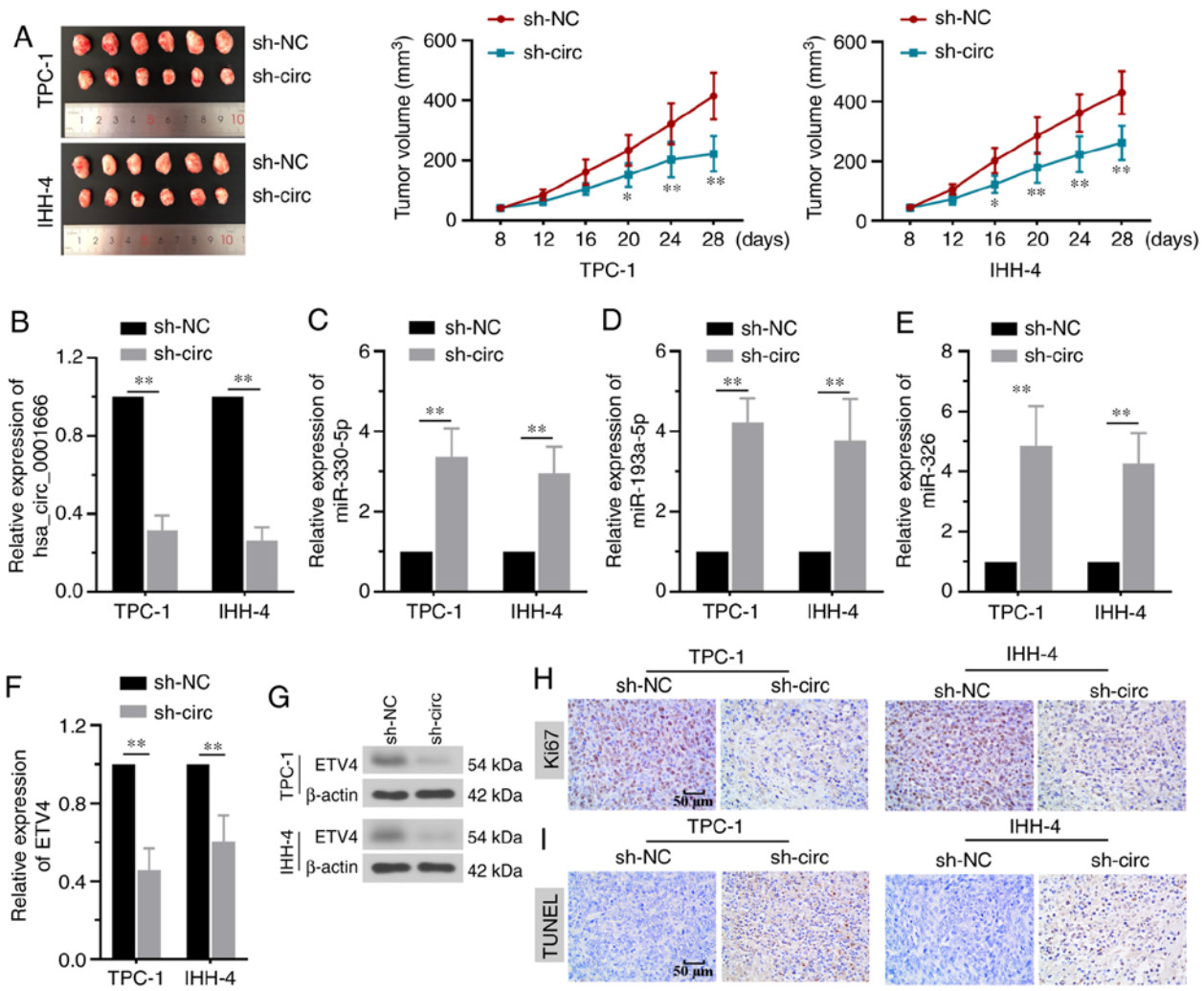

Figure 6. Silencing hsa_circ_0001666 inhibits tumor growth *in vivo*. (A) TPC-1 or IHH-4 cells transfected with sh-NC or sh-hsa_circ_0001666 were subcutaneously injected into nude mice, which were sacrificed 28 days later. Knockdown of hsa_circ_0001666 decreased tumor size. (B) Inhibition of hsa_circ_0001666 expression decreased its expression and increased (C) miR-330-5p, (D) miR-193a-5p and (E) miR-326 expression levels. ETV4 (F) mRNA and (G) protein expression levels were downregulated by hsa_circ_0001666 shRNA. (H) Ki67 expression was decreased by knocking down hsa_circ_0001666, as shown by immunohistochemistry. (I) Apoptosis was increased by hsa_circ_0001666 silencing, as shown by TUNEL staining. *P<0.05, **P<0.01 vs. sh-NC. circ, circular; sh, short hairpin; NC, negative control; miR, microRNA; ETV4, ETS variant transcription factor 4.

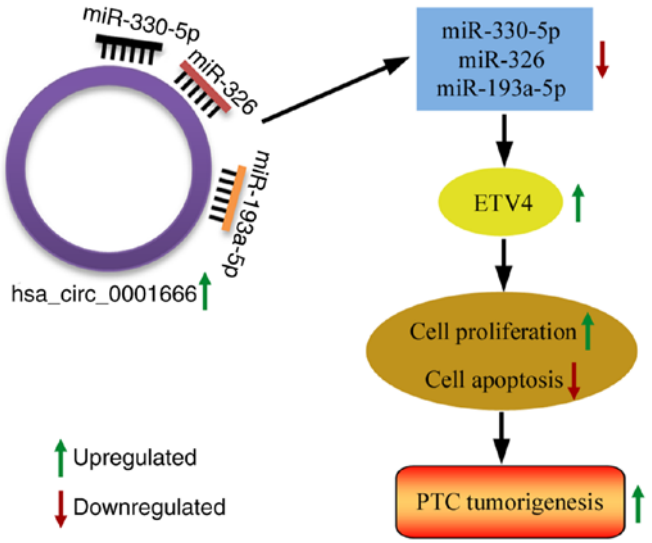

Figure 7. Hsa_circ_0001666 promotes the progression of PTC via regulating the miR-330-5p/miR-193a-5p/miR-326/ETS variant transcription factor 4 pathway. PTC, papillary thyroid carcinoma; miR, microRNA; circ, circular.

in vitro and *in vivo*. However, whether hsa_circ_0001666 improves diagnostic sensitivity and specificity in combination with traditional biomarkers in PTC tumors remains to be determined. In addition, considering the structural specificity of circRNAs, the circRNA overexpressing plasmid is challenging to construct because of the instability of its loop-forming efficiency and accuracy. Thus, the biological functions of circRNAs using both overexpressing and knockdown vectors should be assessed when technology for modulation of circRNA expression has matured. Furthermore, due to the small size of PTC tumors and the emergence of COVID-19, clinical tumors and adjacent normal tissue were difficult to access. Only a limited quantity was obtained to assess the potential association with clinicopathological features. Thus, additional samples should be gathered for further analysis.

In summary, the upregulated expression of hsa_circ_0001666 exhibited an oncogenic role in the malignant behavior of PTC tumors. Hsa_circ_0001666 functioned as a miRNA sponge to inhibit proliferation and enhance apoptosis of PTC cells by positively regulating ETV4. The findings of the present study

highlight the potential role of circRNA hsa_circ_0001666 as a molecular target for PTC diagnosis and treatment.

Acknowledgements

Not applicable.

Funding

The present study was supported by grants from the Science and Technology Planning Project of Shenyang (grant no. 19-112-4-013) and Medical Education Science Research of China Medical University (grant no. YDJK2020042).

Availability of data and materials

The datasets used and/or analyzed during the present study are available from the corresponding author on reasonable request.

Authors' contributions

YQ and JH conceptualized and designed the research. YQ, JH, YZ and LW performed the experiments. YY and BY contributed reagents and collected clinical samples. YQ and ZT analyzed the data. YQ and JH wrote and revised the manuscript. YQ, JH, YY and ZT confirm the authenticity of all the raw data. All authors read and approved the final manuscript and agree to be accountable for all aspects of the research in ensuring that the accuracy or integrity of any part of the work are appropriately investigated and resolved.

Ethics approval and consent to participate

The present study was approved by Shengjing Hospital of China Medical University (approval no. 2019PS322K). All patients provided written informed consent. Animal experiments were approved by Shengjing Hospital of China Medical University (approval no. 2019PS296K).

Patient consent for publication

Not applicable.

Competing interests

The authors declare they have no competing interests.

References

1. Bray F, Ferlay J, Soerjomataram I, Siegel RL, Torre LA and Jemal A: Global cancer statistics 2018: GLOBOCAN estimates of incidence and mortality worldwide for 36 cancers in 185 countries. CA Cancer J Clin 68: 394-424, 2018.
2. Ancker OV, Krüger M, Wehland M, Infanger M and Grimm D: Multikinase inhibitor treatment in thyroid cancer. Int J Mol Sci 21: 10, 2019.
3. Jiang C, Cheng T, Zheng X, Hong S, Liu S, Liu J, Wang J and Wang S: Clinical behaviors of rare variants of papillary thyroid carcinoma are associated with survival: A population-level analysis. Cancer Manag Res 10: 465-472, 2018.
4. Fallahi P, Ferrari SM, Galdiero MR, Varricchi G, Elia G, Ragusa F, Paparo SR, Benvenga S and Antonelli A: Molecular targets of tyrosine kinase inhibitors in thyroid cancer. Semin Cancer Biol 26: S1044-S1579, 2020.
5. Chakravarty D, Santos E, Ryder M, Knauf JA, Liao XH, West BL, Bollag G, Kolesnick R, Thin TH, Rosen N, *et al*: Small-Molecule MAPK inhibitors restore radioiodine incorporation in mouse thyroid cancers with conditional BRAF activation. J Clin Invest 121: 4700-4711, 2011.
6. Jeck WR and Sharpless NE: Detecting and characterizing circular RNAs. Nat Biotechnol 32: 453-461, 2014.
7. Thomson DW and Dinger ME: Endogenous microRNA sponges: Evidence and controversy. Nat Rev Genet 17: 272-283, 2016.
8. Wang F, Nazarali AJ and Ji S: Circular RNAs as potential biomarkers for cancer diagnosis and therapy. Am J Cancer Res 6: 1167-1176, 2016.
9. Ebbesen KK, Kjems J and Hansen TB: Circular RNAs: Identification, biogenesis and function. Biochim Biophys Acta 1859: 163-168, 2016.
10. Yu J, Xu QG, Wang ZG, Yang Y, Zhang L, Ma JZ, Sun SH, Yang F and Zhou WP: Circular RNA cSMARCA5 inhibits growth and metastasis in hepatocellular carcinoma. J Hepatol 68: 1214-1227, 2018.
11. Chen L, Nan A, Zhang N, Jia Y, Li X, Ling Y, Dai J, Zhang S, Yang Q, Yi Y, *et al*: Circular RNA 100146 functions as an oncogene through direct binding to miR-361-3p and miR-615-5p in non-small cell lung cancer. Mol Cancer 18: 13, 2019.
12. Huang Q, Guo H, Wang S, Ma Y, Chen H, Li H, Li J, Li X, Yang F, Qiu M, *et al*: A novel circular RNA, circXPO1, promotes lung adenocarcinoma progression by interacting with IGF2BP1. Cell Death Dis 11: 1031, 2020.
13. Guo D, Li F, Zhao X, Long B, Zhang S, Wang A, Cao D, Sun J and Li B: Circular RNA expression and association with the clinicopathological characteristics in papillary thyroid carcinoma. Oncol Rep 44: 519-532, 2020.
14. Liu W, Zhao J, Jin M and Zhou M: circRAPGEF5 contributes to papillary thyroid proliferation and metastatis by regulation miR-198/FGFR1. Mol Ther Nucleic Acids 14: 609-616, 2019.
15. Peng N, Shi L, Zhang Q, Hu Y, Wang N and Ye H: Microarray profiling of circular RNAs in human papillary thyroid carcinoma. PLoS One 12: e0170287, 2017.
16. Kim HJ, Kim YH, Lee DS, Chung JK and Kim S: In vivo imaging of functional targeting of miR-221 in papillary thyroid carcinoma. J Nucl Med 49: 1686-1693, 2008.
17. Jia M, Shi Y, Li Z, Lu X and Wang J: MicroRNA-146b-5p as an oncomiR promotes papillary thyroid carcinoma development by targeting CCDC6. Cancer Lett 443: 145-156, 2019.
18. Wu G, Zhou W, Lin X, Sun Y, Li J, Xu H, Shi P, Gao L and Tian X: circRASSF2 acts as ceRNA and promotes papillary thyroid carcinoma progression through miR-1178/TLR4 signaling pathway. Mol Ther Nucleic Acids 19: 1153-1163, 2020.
19. Liu F, Yin R, Chen X, Chen W, Qian Y, Zhao Y, Jiang Y, Ma D, Hu T, Yu T, *et al*: Over-Expression of miR-206 decreases the euthyrox-resistance by targeting MAP4K3 in papillary thyroid carcinoma. Biomed Pharmacother 114: 108605, 2019.
20. Gao Y, Wang F, Zhang L, Kang M, Zhu L, Xu L, Liang W and Zhang W: LINC00311 promotes cancer stem-like properties by targeting miR-330-5p/TLR4 pathway in human papillary thyroid cancer. Cancer Med 9: 1515-1528, 2020.
21. Nie FR, Li QX, Wei HF and Ma Y: MiR-326 inhibits the progression of papillary thyroid carcinoma by targeting MAPK1 and ERBB4. Neoplasma 67: 604-613, 2020.
22. Wang Y, Ding X, Liu B, Li M, Chang Y, Shen H, Xie SM, Xing L and Li Y: ETV4 overexpression promotes progression of non-small cell lung cancer by upregulating PXN and MMP1 transcriptionally. Mol Carcinog 59: 73-86, 2020.
23. Chen Y, Sumardika IW, Tomonobu N, Kinoshita R, Inoue Y, Iioka H, Mitsui Y, Saito K, Ruma IM, Sato H, *et al*: Critical role of the MCAM-ETV4 axis triggered by extracellular S100A8/A9 in breast cancer aggressiveness. Neoplasia 21: 627-640, 2019.
24. Tyagi N, Deshmukh SK, Srivastava SK, Azim S, Ahmad A, Al-Ghadhban A, Singh AP, Carter JE, Wang B and Singh S: ETV4 facilitates cell-cycle progression in pancreatic cells through transcriptional regulation of cyclin D1. Mol Cancer Res 16: 187-196, 2018.
25. Tang Q, Chen Z, Zhao L and Xu H: Circular RNA hsa_circ_0000515 acts as a miR-326 sponge to promote cervical cancer progression through up-regulation of ELK1. Aging (Albany NY) 11: 9982-9999, 2019.
26. National Research Council: Guide for the Care and Use of Laboratory Animals. 8th edition. National Academies Press, Washington, DC, 2011.
27. Livak KJ and Schmittgen TD: Analysis of relative gene expression data using real-time quantitative PCR and the 2(-Delta Delta C(T)) method. Methods 25: 402-408, 2001.

28. Chen J, Chen T, Zhu Y, Li Y, Zhang Y, Wang Y, Li X, Xie X, Wang J, Huang M, *et al*: circPTN sponges miR-145-5p/miR-330-5p to promote proliferation and stemness in glioma. J Exp Clin Cancer Res 38: 398, 2019.
29. Wang C, Tao W, Ni S and Chen Q: Circular RNA circ-foxo3 induced cell apoptosis in urothelial carcinoma via interaction with miR-191-5p. Onco Targets Ther 12: 8085-8094, 2019.
30. Gui X, Li Y, Zhang X, Su K and Cao W: Circ_LDLR promoted the development of papillary thyroid carcinoma via regulating miR-195-5p/LIPH axis. Cancer Cell Int 20: 241, 2020.
31. Guan H, Guo Y, Liu L, Ye R, Liang W, Li H, Xiao H and Li Y: INAVA promotes aggressiveness of papillary thyroid cancer by upregulating MMP9 expression. Cell Biosci 8: 26, 2018.
32. Liu F, Zhang J, Qin L, Yang Z, Xiong J, Zhang Y, Li R, Li S, Wang H and Yu B: Circular RNA EIF6 (Hsa_circ_0060060) sponges miR-144-3p to promote the cisplatin-resistance of human thyroid carcinoma cells by autophagy regulation. Aging (Albany NY) 10: 3806-3820, 2018.
33. Ye M, Hou H, Shen M, Dong S and Zhang T: Circular RNA circFOXM1 plays a role in papillary thyroid carcinoma by sponging miR-1179 and regulating HMGB1 expression. Mol Ther Nucleic Acids 19: 741-750, 2020.
34. Afzali F and Salimi M: Unearthing regulatory axes of breast cancer circRNAs networks to find novel targets and fathom pivotal mechanisms. Interdiscip Sci 11: 711-722, 2019.
35. Memczak S, Jens M, Elefsinioti A, Torti F, Krueger J, Rybak A, Maier L, Mackowiak SD, Gregersen LH, Munschauer M, *et al*: Circular RNAs are a large class of animal RNAs with regulatory potency. Nature 495: 333-338, 2013.
36. Zheng Q, Bao C, Guo W, Li S, Chen J, Chen B, Luo Y, Lyu D, Li Y, Shi G, *et al*: Circular RNA profiling reveals an abundant circHIPK3 that regulates cell growth by sponging multiple miRNAs. Nat Commun 7: 11215, 2016.
37. Bibby BAS, Miranda CS, Reynolds JV, Cawthorne CJ and Maher SG: Silencing microRNA-330-5p increases MMP1 expression and promotes an invasive phenotype in oesophageal adenocarcinoma. BMC Cancer 19: 784, 2019.
38. Ghaemi Z, Soltani BM and Mowla SJ: MicroRNA-326 functions as a tumor suppressor in breast cancer by targeting ErbB/PI3K signaling pathway. Front Oncol 9: 653, 2019.
39. Li P, Xiao Z, Luo J, Zhang Y and Lin L: MiR-139-5p, miR-940 and miR-193a-5p inhibit the growth of hepatocellular carcinoma by targeting SPOCK1. J Cell Mol Med 23: 2475-2488, 2019.
40. Xu L, Hu H, Zheng LS, Wang MY, Mei Y, Peng LX, Qiang YY, Li CZ, Meng DF, Wang MD, *et al*: ETV4 is a theranostic target in clear cell renal cell carcinoma that promotes metastasis by activating the pro-metastatic gene FOSL1 in a PI3K-AKT dependent manner. Cancer Lett 482: 74-89, 2020.
41. Xiaohui C, Xin LI and Dehua WU: E26 transformation-specific variant 4 promotes sorafenib and cisplatin resistance in hepatocellular carcinoma cells in vitro. Nan Fang Yi Ke Da Xue Xue Bao 39: 875-882, 2019 (In Chinese).
42. Gupta A, Towers C, Willenbrock F, Brant R, Hodgson DR, Sharpe A, Smith P, Cutts A, Schuh A, Asher R, *et al*: Dual-Specificity protein phosphatase DUSP4 regulates response to MEK inhibition in BRAF wild-type melanoma. Br J Cancer 122: 506-516, 2020.